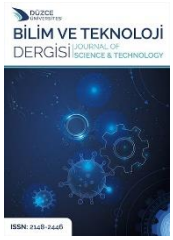

Düzce University
Journal of Science & Technology

https://dergipark.org.tr/tr/pub/dubited

Research paper

Effect of Colemanite Concentrator Waste (CW) Substitution in Cement-Based Mortars on the Gamma-Ray Shielding Performance, Mechanical and Physical Properties

Şevki Eren[a,*], *Doğan Yaşar*[b], *Selahattin Güzelküçük*[c], *Gökhan Ekincioğlu*[d], *Yunus Karataş*[e]

[a]Department of Construction Technology, Vocational School, Kırşehir Ahi Evran University, Kırşehir, Türkiye
[b]Department of Physics, Faculty of Arts and Sciences, Kırşehir Ahi Evran University, Kırşehir, Türkiye
[c]Department of Architecture and Urban Planning, Ayaş Vocational School, Ankara University, Ankara, Türkiye
[d]Department of Mining and Extraction, Kaman Vocational School, Kırşehir Ahi Evran University, Kırşehir, Türkiye
[e]Department of Chemistry, Faculty of Arts and Sciences, Kırşehir Ahi Evran University, Kırşehir, Türkiye
***Corresponding author:** seren@ahievran.edu.tr

Article information:
Received: 13/05/2025, Revision: 07/08/2025, Accepted: 02/09/2025
DOI: 10.29130/dubited.1695973

ABSTRACT

This study investigates the influence of colemanite concentrator waste (CW) as a cement substitute on the gamma-ray shielding performance, mechanical, and physical properties of mortars. Mortar mixtures were prepared with varying CW proportions, and their consistency, setting time, compressive strength, pulse velocity, and water absorption were determined. Microstructural analysis using SEM and experimental gamma-ray (Cs-137-662 keV) shielding tests were also conducted.

Results indicate that increasing CW substitution generally led to decreased compressive strength and increased total water absorption, consistency, and setting time. Notably, mixtures with CW content exceeding 5 wt% experienced disintegration during curing, primarily attributed to the significant retardation of cement hydration by boron compounds. For radiation shielding, despite the lower density of CW influencing overall bulk density, the presence of higher atomic number elements in colemanite demonstrated a positive contribution to gamma-ray attenuation. Specifically, at the lowest material thicknesses, the lead equivalent levels for CW2.5 and CW5 mortars were measured as 0.64 mmPb and 0.70 mmPb, respectively, revealing a clear radiation attenuation effect compared to the control. These findings highlight the potential of colemanite concentrator waste as a promising lead-free material for radiation shielding applications in cement-based composites.

Keywords: *Colemanite Concentrator Waste, Radiation Shielding, Gamma-Ray Shielding, Compressive Strength, Cement-Based Mortar*

I. INTRODUCTION

It is commonly known that ionizing radiation is hazardous to human health, and that shielding techniques, time, and distance can protect against such radiation sources (Khan & Gibbons, 2014; International Atomic Energy Agency, 2011; International Commission on Radiological Protection, 2007).

Factors such as atomic mass number, density, thickness, cross-section, and photon energy affect the attenuation properties of shielding materials (Ersundu et al., 2018). Many substances, each with special qualities, can be utilized to shield against radiation, including water, iron, lead, compact soil, regular and heavyweight concrete, and iron (Ouda, 2015; El-Sayed Abdo, 2002; Rezaei-Ochbelagh & Azimkhani, 2012). Radiation shielding concrete is a high-density concrete that prevents possible leakage of X-rays, gamma rays, and fast-moving neutrons in various establishments such as nuclear power structures in hospitals, X-ray or radiology department rooms (Tyagi et al., 2020). It is the most widely used shielding material because it is inexpensive, easy to mold, and suitable for neutron shielding (Han et al., 2017). The focus on developing various concrete mixtures and utilizing various additives has recently increased in tandem with the growing interest in radiation-shielding concrete mixtures (Al-Saadi & Saadon, 2014; Saudi, 2013; Kavaz et al., 2019). Due to its wide availability and low cost, colemanite has been explored for inclusion in ordinary cements and mortars, lightweight concretes, bricks, and geopolymers as an aggregate or binder, and its usability in radiation shielding concrete continues to be explored by the authors (Lotti et al., 2019). Turkey possesses significant boron reserves, with its mining operations generating approximately 250 million tons of boron-containing waste annually. The utilization of these boron mineral wastes, particularly in the cement and concrete industry, holds considerable importance for environmental sustainability (Ustabas, 2024). The results of the research conducted in the literature on the gamma-ray attenuation performance of colemanite concentrator wastes in cement-based composites are given below.

Özturk et al. (2020) investigated the mechanical and radiation shielding properties of alkali-activated cement mortar mixtures (AAC) prepared by using different precursors such as ground granular blast furnace slag (GGBFS), fly ash (FA), metakaolin (MK), and boron-containing waste clay material (WCB). They reported that the WCB and MK-incorporating AAC mixtures have slightly worse gamma attenuation properties than the ordinary portland cement (OPC). In addition, the compressive strengths of the colemanite-substituted AAC2 (WCB 100%) and AAC3 (50% GGBFS and 50% WCB) mixtures were lower than the OPC. Binici et al. (2014) investigated the mechanical and radiation shielding properties of cement-based mortars containing standard sand aggregate, which they prepared by substituting colemanite, barite, ground basaltic pumice, and GGBFS as an additive for cement. They determined that the colemanite-added mortars had low radiation permeability. As the colemanite ratio increased, the compressive strengths decreased compared to the reference mixtures. Moreover, research consistently indicates that the incorporation of boron minerals or their waste generally leads to a decrease in the compressive strength of cementitious materials. This aligns with observations by Ustabas (2024), who similarly reported reduced compressive strength in cement with boron mineral additions. Yaltay et al. (2015) investigated the radiation shielding properties and the effect of curing ages on the radiation shielding of lightweight concrete containing different proportions of pumice aggregate produced by substituting colemanite for cement at 0-2%. They reported that the radiation shielding properties of 28-day lightweight concrete can be improved when 0.4%-2% colemanite is substituted for cement. In addition, 2% and 6% colemanite ratios delayed the initial setting times in the trial mixtures. Demir et al. (2011) made measurements of 663 keV gamma-rays in a Cs137 radiation source, using the beam transmission method of concrete produced with barite, colemanite, and normal aggregate. They reported that the linear attenuation coefficient decreased with the colemanite concentration and increased with the barite concentration. Oto et al. (2013) evaluated the radiation shielding properties of concretes containing 0-20% of barite and colemanite aggregates. They revealed that concretes containing barite and colemanite are more effective at attenuating gamma rays than the ordinary concretes. Furthermore, studies on radioactive permeability, including that by Ustabas (2024), suggest that while boron's low atomic number can be beneficial for neutron shielding, it also demonstrates effectiveness in attenuating gamma rays. Specifically, colemanite has been observed to improve gamma-ray attenuation in concrete. Oto et al. (2019) investigated the gamma and fast neutron shielding parameters of concretes with and without colemanite mineral additives. Instead of ordinary aggregate, colemanite mineral was added at the rates of 0-20% by weight. They observed that concretes with colemanite minerals are not very effective in gamma radiation shielding. However, they determined that the compressive strength increased up to a 10% colemanite ratio, but decreased after a 10% colemanite ratio. Yadollahi et al. (2016) used the Taguchi method and an artificial neural network to create the optimum mix design of concrete containing colemanite aggregate. They reported that boron additives significantly delay the setting time and reduce the compressive strength. Consistent with these findings, Ustabas (2024) further demonstrated that boron minerals significantly extend the initial setting time of cement, with higher concentrations of B_2O_3 (e.g., above 0.6%) causing a pronounced increase in setting times. Demir and Keleş (2006) calculated the mass attenuation coefficients of concretes containing borogypsum and CW. Clinker,

cement, and modular sand were used in the experiments. Cement mortar samples were obtained by adding CW samples to clinker at the rates of 0-15% by weight. They stated that the borogypsum and CW are useful in stopping the spread of radiation and can be utilized in cement mortars as gamma-ray shielding materials.

Upon analyzing the aforementioned literature studies, it is observed that certain concretes containing colemanite improve the attenuating gamma rays (Ustabas, 2024; Binici et al., 2014; Yaltay et al., 2015; Oto, Gür, et al., 2013; Demir & Keleş, 2006), while other studies report no discernible improvement (Özturk et al., 2020; Demir et al., 2011; Oto et al., 2019). In this context, there are differences in the literature results. The objective of this research is to evaluate the compressive strength, pulse velocity, setting time, consistency, and microstructure tests in addition to investigating the attenuating effects of gamma rays against the ionizing radiation of colemanite concentrator wastes experimentally and through an interdisciplinary study. The present study provides important technical support for the use of CW in cement-based mortars.

II. MATERIALS AND METHODS

A. Materials

The cement mortars were produced by Portland cement (CEM I 42.5 R), CW powders, standard sand (conforming to TS EN 197-1), and tap water. CW (specific gravity: 2.43 g/cm^3) was supplied by Emet Boron Operations Directorate Emet/Kütahya/Türkiye. The chemical composition of the Portland cement (specific gravity: 3.11 g/cm^3) and CW micro-particles is given in Table 1. The calcination process visual of CW is given in Figure 1. The particle size distribution of CW and cement powders obtained by the laser diffraction technique is presented in Figure 2. As can be seen from Figure 2, cement particle sizes are finer than CW, generally ranging from 0.001 µm to 98.71 µm. Cement's d10, d50, and d90 grain diameter values are 1.99 µm, 18.91 µm, and 49.23 µm, respectively. The particle sizes of CW powders vary between 1.65 µm and 1260 µm, with d10, d50, and d90 grain diameter values being 72.6 µm, 157 µm, and 366 µm, respectively. The d50 value of cement is 18.91 µm, while the d50 value of CW is 157 µm.

Table 1. Chemical composition of Portland cement and CW, wt-%

Materials	CaO	SiO_2	Al_2O_3	Fe_2O_3	MgO	Na_2O	K_2O	SO_3	B_2O_3	SrO	Others
CEM I 42.5 R	62.02	17.46	3.56	3.31	1.43	0.29	1.07	3.96	-	-	6.9
CW	22.6	23.4	4.15	1.85	4.16	0.34	2.61	0.48	36.97	1.11	2.33

before calcination calcination process of CW after calcination

Figure 1. Calcination process visual of CW.

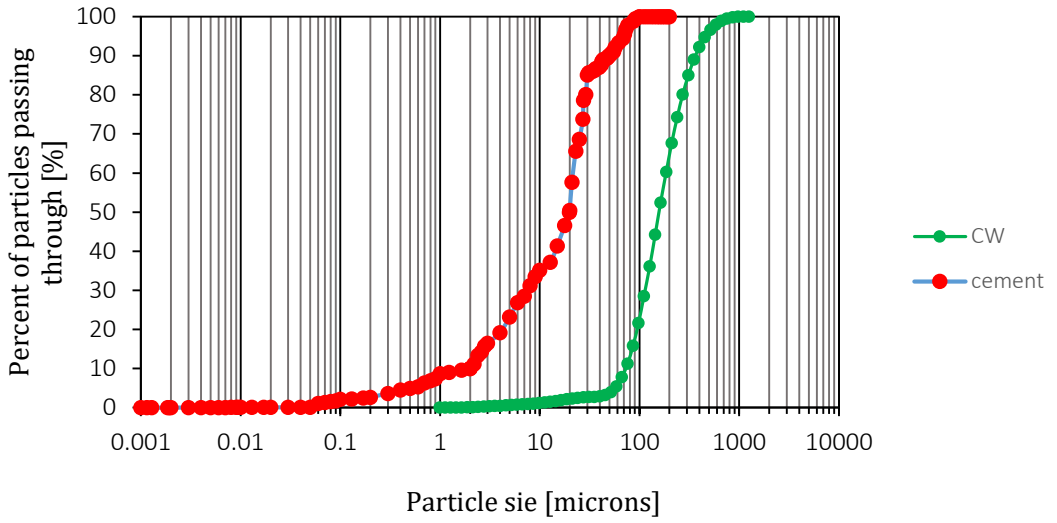

Figure 2. Particle size distribution of CW and cement powders.

A. 1. Mixture Compositions

The cement mortars (conforming to ASTM C 109) were produced with a water-to-binder fixed ratio of 0.485 and a sand-to-binder fixed ratio of 2.75. In total, seven series of mortars were produced, including a control cement mortar. Six series of mortars containing 2.5, 5, 7.5, 10, 15, and 20 wt-% CW as cement replacement were produced and these parts were designated as CW 2.5, CW 5, CW7.5, CW 10, CW 15, and CW 20, respectively. To provide the transition from a crystalline structure to an amorphous one, CW was calcined at 800 degrees for two hours and grounded. This thermal treatment is essential as it enhances the reactivity of the colemanite waste, making it more suitable for its intended use as a cement substitute by improving its binding properties. The number next to the letter indicates the percentage of CW powders used as a cement substitute by weight. The mixture composition of the cement mortars is presented in Table 2.

Table 2. Cement mortar mixture design.

Mortar mixtures	Sand [g]	Cement [g]	Water [g]	CW		water/ binder
				[wt-%]	[g]	
C0	1350	491	238	-	-	0.485
CW2.5	1350	478.725	238	2.5	12.275	0.485
CW5	1350	466,45	238	5	24.55	0.485
CW7.5	1350	454.175	238	7.5	36.825	0.485
CW10	1350	441.9	238	10	49.1	0.485
CW15	1350	417.35	238	15	73.65	0.485
CW20	1350	392.8	238	20	98.2	0.485

A.2. Mixing Procedure and Testing Methods

The test standards, equations, and specifications performed in the current study are given in Table 3. Five specimens were prepared and tested for each mixture and curing time.

Table 3. Test standards, equations, and specifications.

Tests	**Stadards**	**Equation/Specifications**
Preparing mortar mixtures	ASTM C 305-06	-
Consistency	ASTM C 1437-07	$\% = (A/D_o)x100$, where $\%$ is the flow in percent, (D_0) is the original inside base diameter in millimeters, A is the average of four readings in millimeters, minus the original inside base diameter (D_0) in millimeters.
Compressive strength (7th and 28th days curing); 50mm cube molds	ASTM C 109	$f_m = P/A$, where f_m is compressive strength (MPa), P is the total maximum load (N), and A is the area of the loaded surface (mm^2).

Table 3 (cost). Test standards, equations, and specifications.

Pulse velocity	ASTM C 597-09	$V=L/T$, where V is the pulse velocity (m/s), L is the distance between centers of transducer faces (m), and T is the transit time (s).
Capillary water absorption (28th-day curing); 50mm cube molds; weight gains of the specimens (0.25h, 1h, 4h, and 24h)	ASTM C 1403	$A_T = (W_T - W_o)x10000/(L_1xL_2)$, where A_T is the water absorption in grams/100 cm^2, W_T is the weight of the specimen at time T in grams, W_0 is the initial weight of the specimen in grams, L_1 is the average length of the test surface of the cube specimen in mm, and L_2 is the average width of the test surface of the cube specimen in mm.
Total water absorption, (28th-day curing; 50mm cube molds)	ASTM C 642	Absorption after immersion: $\% = [(B - A)/A]$x100, where A is the dry weights of the specimens, B is the dry surface saturation weights.
Setting time	TS EN 196-3	-

A.3. Measurement of Lead Equivalent Thickness of Cement-Based Mortars in Gamma Radiation

For the mortar samples to be used in radiation attenuation experiments, molds with 100 mm diameter and 5, 10, 20, and 30 mm thickness were prepared. The mortars were compressed into the molds in two layers. The exact thickness of each concrete mixture sample was determined and noted using a micrometer. Radiation attenuation experiments were carried out in the standard calibration laboratory at Ankara University Institute of Nuclear Sciences in accordance with the IEC 61331-1: 2014 – 05 standard (The International Electrotechnical Commission, 2014), in a Cs-137 (662 keV) gamma radiation beam. The radiation attenuation curve in the lead filter was obtained at the energy quality specified above using lead filters with 99.9% purity and different thicknesses between 0.15 mmPb and 1.5 mmPb. The radiation transmittance of the produced mortar samples was measured at the radiation energy and irradiation geometries specified above. The attenuation amounts and lead equivalent thicknesses of the mortar samples were determined using the equation of standard lead exponential curves. Cs-137 gamma irradiation system; In the radiation attenuation tests of mortar samples, Hopewell Design Gamma irradiation unit G10 model, a system containing 2 Cs-137 sources with nominal activities of 50 mCi and 10 Ci was used. Mortar samples and standard filters were placed on a bench that provided 3-dimensional movement between the radiation source and the detector, and measurements were performed. In the radiation measurements, a PTW trademark 30 cm^3 spherical ion chamber and a PTW Unidose Webline dose rate reading system calibrated in the secondary standard dosimetry laboratory were used. The irradiation system and test measurement setup are shown in Figure 3. The visual of the samples produced to determine the radiation shielding properties is presented in Figure 4.

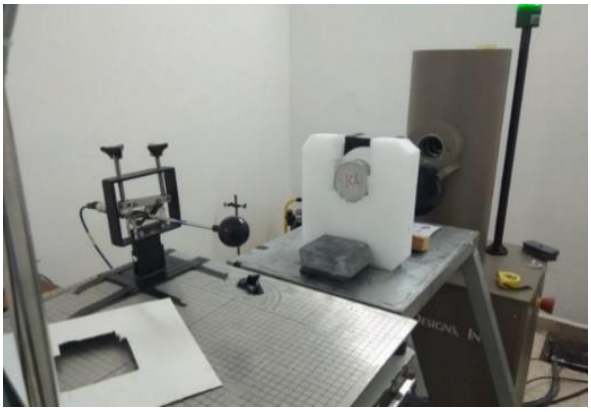

Figure 3. Cs-137 gamma irradiation system and geometry.

Placing radiation samples into the mold

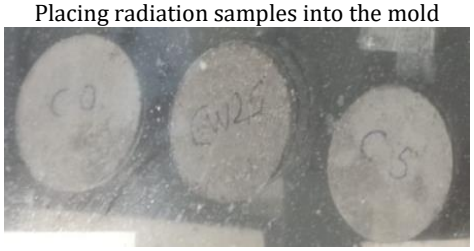

Keeping radiation samples in the curing pool (28 days)

Radiation samples taken from the curing pool

Figure 4. The visual of the samples produced for radiation shielding.

III. RESULTS AND DISCUSSION

The visual of the samples placed in the curing pool is shown in Figure 5. It was observed that the samples did not harden sufficiently due to insufficient hydration at CW substitutions above 5% (7.5%, 10%, 15%, and 20%), and these samples were seen to disperse when placed in the curing pool.

In the study conducted Aksoğan et al. (2016), ettringite formations in the C–S–H structure were reported in samples containing colemanite. Some other researchers (Mutuk & Mesci, 2014; Olgun et al., 2007) reported that needle-like hydration products were encountered in SEM analyses due to the use of colemanite. When the CH crystals detected in the images were examined, it was observed that the typical hexagonal structure of these crystals was disrupted. Kavas et al. (2007) stated that the morphology of portlandite crystals in cement pastes containing colemanite may be slightly different. As a result, this situation may weaken the binding properties of the mortar. In the current study, when the setting time results in Table 4 are examined, the setting times of mixtures containing high CW content, such as CW10, CW15, and CW20, are determined to be "non-standard," a clear indication that hydration is excessively delayed or halted by the effects of boron. This is considered the primary mechanism that causes the samples to fail to harden sufficiently during curing, resulting in fragmentation and, consequently, strength loss, even when the setting times are within the standard values (e.g., for CW7.5). This significant delay is also supported by the findings of Ustabas (2024), who reported that even small amounts of colemanite prolong the initial setting time and reduce the heat of hydration of the cement. This can be directly related to the insufficient hardening and fragmentation of the samples observed at higher CW replacements. Therefore, the disintegration of samples containing high proportions of CW is directly related to the chemical retarding effect of boron and its negative effect on hydration kinetics rather than the increased effective water-binder ratio.

In all tests performed with CW substitution, only CW2.5 and CW5 mixtures could be examined. The findings of all tests conducted within the scope of the study are explained in detail below.

Figure 5. Visual of samples placed in the curing pool.

A. Consistency

The flow percentage values of the mortar mixtures are shown in Figure 6.

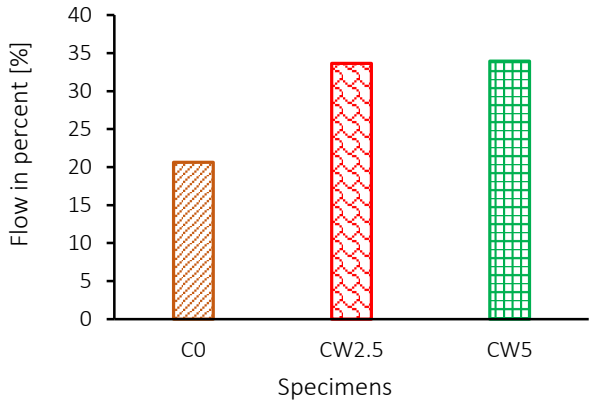

Figure 6. Flow percentage values of mortar mixtures.

As seen in Figure 6, the flow percentage of the control mortar mixture is determined to be 20.63% and the flow percentage values increase with increasing CW substitution. The increase rate in the flow percentage value of CW2.5 and CW5 samples is 63.08% and 64.62%, respectively. Workability is positively affected by increasing CW substitution. This observed increase in flow is likely attributed to the coarser particle size distribution of CW compared to cement, as clearly illustrated in Figure 2. The larger average particle sizes of CW (e.g., CW's d50 is 157 µm compared to cement's 18.91 µm) imply a lower specific surface area, which can reduce the overall water demand of the mixture, thereby enhancing its fluidity and increasing the flow percentage for a given water-to-binder ratio.

B. Setting Time

All mixtures' setting time tests were determined using the Vicat apparatus. The setting time results of the mortar mixtures are shown in Table 4.

Table 4. Setting times of the mortar mixtures.

Mortar mixtures	Initial setting time, (min)	Final setting time, (min)
C0	220	295
CW2.5	245	300
CW5	260	345
CW7.5	285	375
CW10	410	out of standard
CW15	out of standard	out of standard
CW20	out of standard	out of standard

Notably, for CW contents above 5 wt% (CW10, CW15, and CW20), the setting times were determined to be 'out of standard', clearly indicating a significant retardation or complete inhibition of cement hydration This phenomenon, primarily caused by boron compounds in colemanite, leads to insufficient hardening and, consequently, the disintegration observed in these high-substitution mixtures (Ustabas, 2024; Yaltay et al., 2015; Yadollahi et al., 2016).

C. Total and Capillary Water Absorption

The total water absorption and capillary water absorption values of the specimens at 28 days are shown in Figure 7 and Figure 8, respectively.

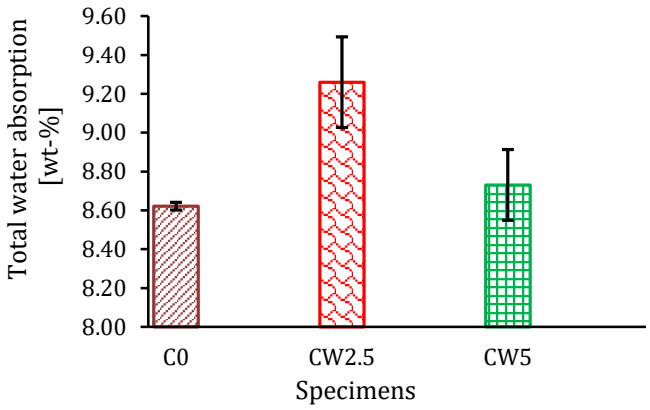

Figure 7. Total water absorption percentages of the specimens by weight on the 28th day.

An indication of increased porosity in the material is a rise in the total water absorption value. When Figure 7 is examined, it is seen that the total water absorption values of CW substituted mixtures are higher than C0. CW2.5 samples' total water absorption values increase by 7.4% compared to C0, while this increase rate is 1.27% in the CW5 samples. The 28-day bulk specific gravity (BHA) values of the hardened mortar specimens were determined as 2.07 g/cm^3 for C0, 2.04 g/cm^3 for CW2.5, and 2.06 g/cm^3 for CW5. These BHA values generally correlate with the observed total water absorption trends, where lower BHA for CW2.5 indicates a slightly less dense and potentially more porous structure compared to C0 and CW5, consistent with its higher total water absorption. The overall higher total water absorption in CW-substituted mixes compared to the control suggests an increased general porosity within the matrix.

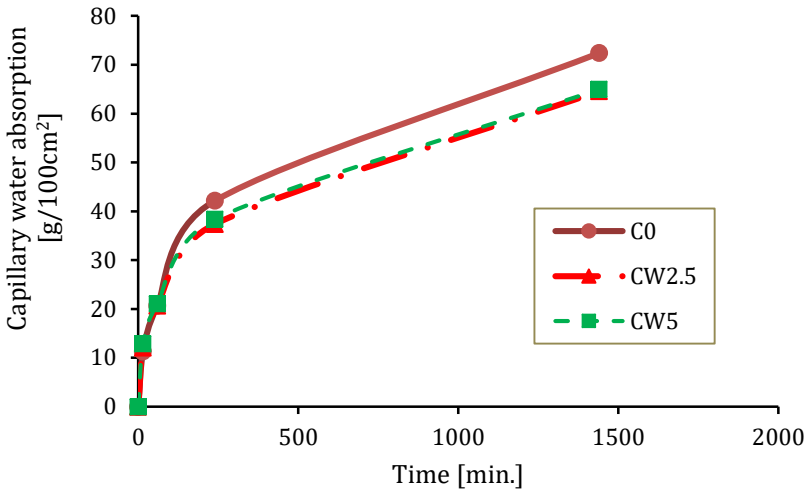

Figure 8. Capillary water absorption values of specimens on the 28th day.

Figure 8 shows that the capillary water absorption values increase with time in all mixtures. However, it is seen that the CW samples' capillary water absorption values are almost the same as each other and are lower than those of the control mixture. Since the structure of the macro and micro voids and capillary voids in the internal structure of the samples is different, the results obtained from the graphs in Figure 7 and Figure 8 may sometimes not be consistent. The capillary pore size, pore size distribution, the connection status of the pores, and other parameters that influence the capillary water absorption behavior may be the cause of the decline in capillary water absorption (Castro et al., 2011). The porous structure of hydrated cement paste is in the nano and micro size range. These spaces between the C-S-H layers create capillary channels, which are irregularly shaped, linked, and have a tendency to shut with hydrated products over time. They are created as the mixing water moves away from the structure. The closure of these channels results in a decrease in permeability (Mehta & Monteiro, 2006). In addition, the fact that the void ratio of CW2.5 substituted mixtures is higher than CW5 may initially give the impression that the strength of CW2.5 substituted mixtures should be lower. However, considering that lower amounts of cement are used in CW5 substituted mixtures, it is considered a normal result that the compressive strength of CW5 substituted mortars is lower than that of CW2.5 mixtures due to slower hydration.

D. Compressive Strength and Pulse Velocity

The compressive strengths and pulse velocities of the specimens on 7 and 28 days are presented in Figure 9.

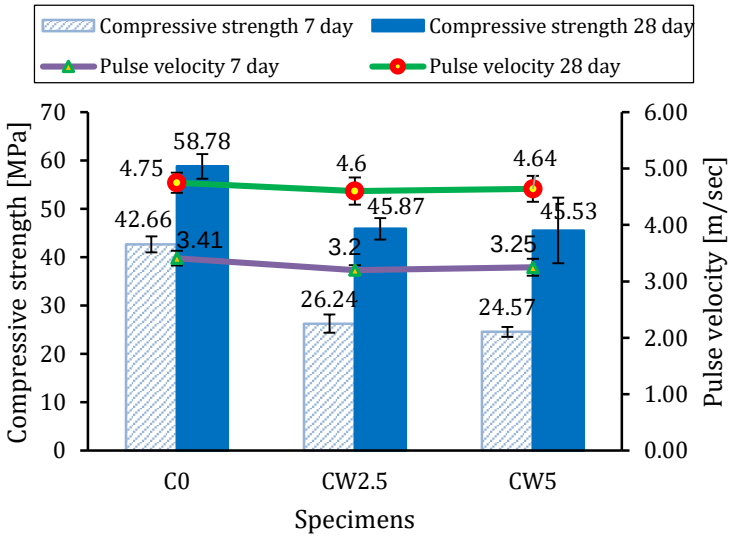

Figure 9. Compressive strengths and pulse velocity values of the specimens on the 7 and 28th days.

As seen in Figure 9, with increasing substitution of CW, both compressive strengths and pulse velocity values decrease compared to C0. In this context, compressive strengths and pulse velocity values are compatible with each other. CW2.5 and CW5 mixtures' 28-day compressive strength loss is 21.96% and 22.54%, respectively. CW2.5 mixtures' 7-day compressive strength value is 42.79% of their 28-day compressive strength. CW5 mixtures' 7-day compressive strength value is 46.03% of their 28-day compressive strength.

In the present study, strength loss in CW-substituted mixtures seems to agree with the works by (Ustabas, 2024; Öztürk et al., 2020; Binici et al., 2014; Yadollahi et al., 2016). However, Oto, Madak et al. (2019) determined that the compressive strength increased up to a 10% colemanite ratio, but decreased after a 10% colemanite ratio. In the current study, the fact that the CW mixtures' total water absorption values are higher than the control mixtures indicates that these mixtures have a more porous structure and therefore emerge as one of the reasons for the loss of strength. This aligns with the observed bulk specific gravity values, where lower densities generally correlate with increased porosity and reduced mechanical performance.

As previously discussed in the 'Total and Capillary Water Absorption' section, while total water absorption generally increases with CW addition, suggesting higher overall porosity, the capillary water absorption exhibits a different trend, potentially due to alterations in the pore network and hydration product morphology induced by colemanite (Castro et al., 2011). Despite variations in capillary absorption, the observed decrease in compressive strength is primarily attributed to the increased overall porosity indicated by total water absorption and colemanite's tendency to slow down cement hydration, as well as the reduced cement content in the mixture due to CW substitution (Mehta & Monteiro, 2006). Furthermore, the replacement of colemanite for cement resulted in a decrease in the mixture's cement content as well as a decrease in strength due to colemanite's tendency to slow down hydration.

E. Microstructural Analysis

SEM images of samples C0, CW2.5, and CW5 are presented in Figures 10a, 10b, and 10c, respectively, and the microstructure analyses are explained. One image, 5µm in size, is given for each specimen.

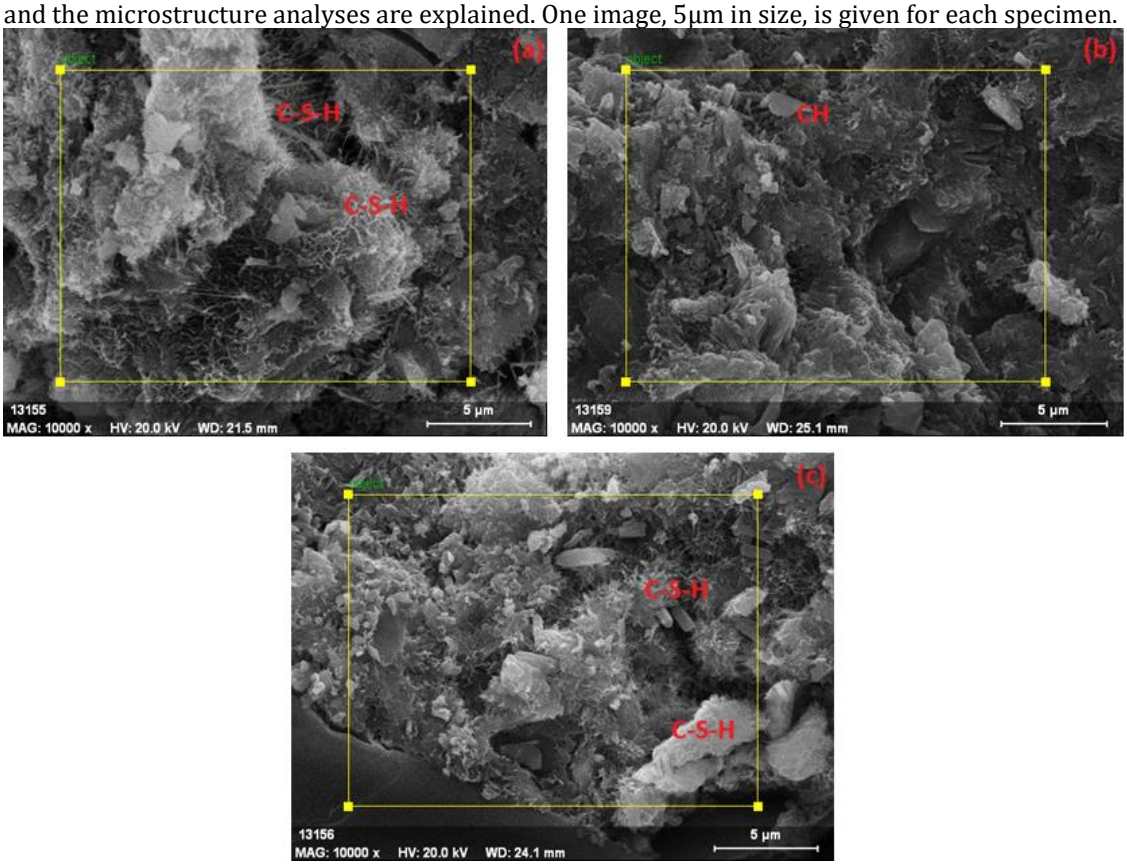

Figure 10. SEM images of a) C0 specimen, b) CW2.5 specimen, c) CW5 specimen.

CH and C-S-H gels are found in all samples, and in some areas, it is observed that the C-S-H gels started to cover the CH crystals. Further examination of the SEM images reveals more specific microstructural characteristics related to CW substitution. In CO specimens (Figure 10a), a relatively denser and more homogeneous matrix with well-formed C-S-H gel and distinguishable CH crystals is observed, indicating efficient hydration. In contrast, CW2.5 (Figure 10b) and especially CW5 (Figure 10c) specimens, despite showing the presence of C-S-H and CH, exhibit signs of a less compact and potentially more porous structure. The morphology of CH crystals appears less defined, and the C-S-H gel seems to form a looser network in CW-substituted samples compared to the control. This observation is consistent with the known retarding effect of boron compounds (from colemanite) on cement hydration, which can lead to a less refined and more open pore structure, thereby contributing to the observed increase in total water absorption and decrease in compressive strength in CW-modified mortars.

Specifically, the presence of needle-like formations observed in similar studies and alterations in the typical hexagonal structure of CH crystals due to colemanite incorporation, as documented in the literatüre (Aksoğan et al., 2016; Mutuk & Mesci, 2014; Olgun et al., 2007) further supports our findings of an altered microstructure and its impact on mechanical performance and porosity. Similar microstructural alterations have been reported by (Ustabas, 2024), where SEM images of colemanite-containing cement pastes revealed distinct formations, including thin needle-like structures, further substantiating the impact of boron on hydration product morphology and overall matrix development. While these specific features are not explicitly detailed in these particular images, the overall textural differences align with the macroscopic properties and the reported effects of boron on cementitious systems.

F. Radiation Attenuation

Radiation attenuation tests were carried out in a standard calibration laboratory. For this purpose, relatively high energy Cs-137 (662 keV) gamma radiation was used, IEC 61331-1:2014–05 (The International Electrotechnical Commission, 2014; ISO 4037-1:2019 (International Organization for Standardization, 2019). To determine the effect of CW on radiation attenuation, C0 coded samples without CW were tested first, followed by CW coded samples containing 2.5 wt% and 5 wt%. Gamma radiation attenuation curves of mortar mixtures exposed to Cs-137 (662 keV) gamma radiation are given in Figure 11 and lead equivalent thickness values are given in Table 5.

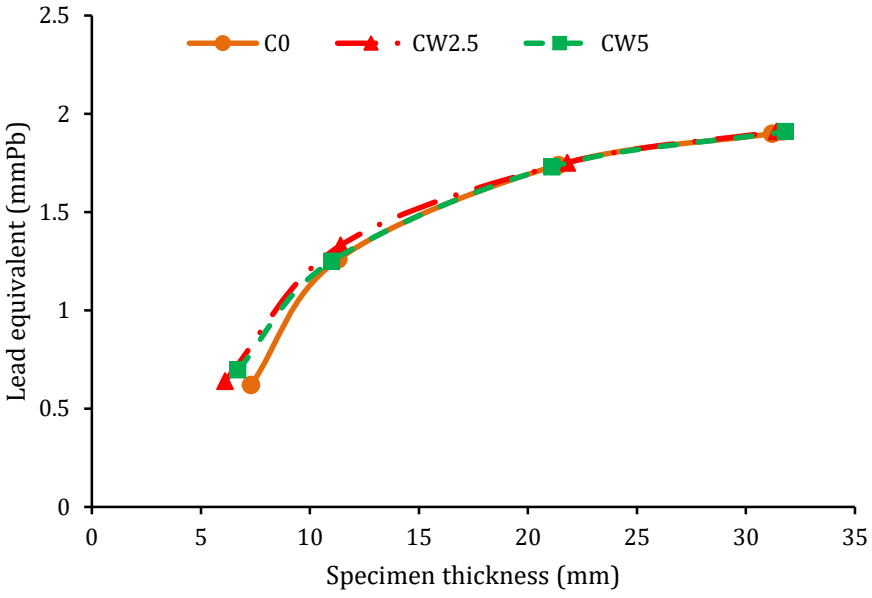

Figure 11. Lead equivalent thickness values of mortar mixtures for Cs-137 (662keV) gamma radiation.

Table 5. Lead equivalent thickness values of mortar samples in Cs-137 gamma ray energy

Serial number	C0		CW2.5			CW5		
	Sample thickness (mm)	Gamma-ray energies Cs-137 (mmPb)	Sample thickness (mm)	Gamma-ray energies Cs-137 (mmPb)	CW2.5/C0 %	Sample thickness (mm)	Gamma-ray energies Cs-137 (mmPb)	CW5/C0 %
1	7.3	0.62	6.1	0.64	1.032	6.7	0.696	1.123
2	11.3	1.26	11.4	1.33	1.056	11	1.25	0.992
3	21.4	1.74	21.8	1.75	1.006	21.1	1.73	0.994
4	31.2	1.9	31.4	1.91	1.005	31.8	1.91	1.005

As seen in Table 5, although the materials with and without colemonite additives are tried to be produced in the same thickness, there are some differences, but the obtained data are at a comparable level. While the quantitative differences in lead equivalent levels for higher thicknesses (e.g., 21.4 mm and 31.2 mm) are small and require further statistical validation, the data obtained at the lowest thickness (around 6-7 mm) clearly reveal the radiation attenuation potential of colemonite additive. For instance, the undoped material (7.3 mm) yielded 0.62 mmPb, whereas CW2.5 (6.1 mm) showed 0.64 mmPb and CW5 (6.7 mm) showed 0.70 mmPb. This initial observation suggests that lead equivalent levels increase linearly with increasing mortar thickness. However, the fact that the colemonite ratio remains low with increasing mortar thickness masks the radiation attenuation effect of colemonite additive.

The radiation shielding performance of a material is inherently linked to its density and microstructural characteristics. In this study, the bulk specific gravity (BHA) values were observed as 2.07 g/cm^3 for C0, 2.04 g/cm^3 for CW2.5, and 2.06 g/cm^3 for CW5. Although the BHA values show slight variations, they are generally comparable across the tested mixes, indicating that bulk density alone may not be the primary factor for the observed differences in radiation attenuation, especially at low substitution levels. However, as previously discussed, CW incorporation leads to an increase in total water absorption (Figure 7), suggesting a more porous structure. Furthermore, microstructural analyses (Figure 10) revealed a less compact C-S-H network and altered CH morphology in CW-substituted samples. Despite these changes suggesting increased porosity, the observed radiation attenuation, particularly at the lowest thicknesses, indicates that the higher atomic number elements present in colemanite (such as Boron, and also higher SiO_2, Al_2O_3, K_2O in CW compared to Cement as seen in Table 1) contribute positively to gamma-ray interaction mechanisms, potentially counteracting the negative effects of increased porosity on shielding capacity. This highlights the complex interplay between material density, microstructural features, and elemental composition in determining overall radiation shielding effectiveness.

IV. CONCLUSION

The present study assesses the potential benefits of incorporating CW into cement-based mortars to create a lead-free shielding material against ionizing radiation, including gamma-ray beams. A comparative study of mortar mixtures with and without CW replacement is conducted in terms of physical, mechanical, and radiation shielding performance. The aforementioned experimental findings allow for the following deductions to be made:

- The increasing CW substitution significantly affects workability by increasing the consistency of the mortars. This is attributed to the particle morphology and surface area of CW, which may alter the water demand and flow characteristics of the fresh mixture.

- All CW substituted specimens' total water absorption percentage by weight is higher than the control specimen. In addition, 7 and 28-day compressive strength and pulse velocity values decrease with increasing CW substitution. The fact that the CW combinations' total water absorption values are higher than the control mixtures indicates that these mixtures have a more porous structure and therefore emerge as one of the reasons for the loss of strength. Moreover, the strengths decrease due to a number of variables, including the tendency of colemanite to slow down hydration and the decrease in cement in the mixture as a result of the CW substitution. Furthermore, at CW substitution rates above 5 wt%, the mortars

experienced disintegration during curing. This is primarily attributed to the significant retardation or inhibition of cement hydration by boron compounds in colemanite, as evidenced by 'out of standard' setting times (Table 4) for higher substitution rates. This chemical interference leads to insufficient hardened matrix formation and subsequent strength loss and disintegration.

• The present study reports that the lead equivalent levels of CW-added materials and control samples with similar thickness are significantly different from each other. In the Cs-137 gamma energy, which is penetrating radiation, the lead equivalent levels of the mortar with 2 different rates of CW added for the lowest thickness are found to be 0.64 mmPb and 0.70 mmPb. It is also seen that the lead equivalent levels increase linearly depending on the mortar thickness. While the current experimental setup provides valuable insights into the potential of CW as a radiation shielding material, particularly at low thicknesses where a clear attenuation effect is observed, the statistical significance of the radiation attenuation data could be further enhanced with a larger number of repeated measurements. Based on the observed trends, we can suggest that CW contributes to radiation retention in low-thickness mortar mixtures, showing promise for lead-free shielding applications. Our findings regarding enhanced radiation attenuation align with (Ustabas, 2024), who also concluded that the addition of colemanite and ulexite increased the linear attenuation coefficient of mortar, thereby decreasing its radioactive permeability. Despite the substitution of lower-density colemanite for higher-density cement, which influences the overall bulk density of the mortar (e.g., C0: 2.07 g/cm^3, CW2.5: 2.04 g/cm^3, CW5: 2.06 g/cm^3), our findings suggest that the higher atomic number elements (such as Boron, SiO_2, Al_2O_3, K_2O in CW) within colemanite waste enhance gamma-ray interaction mechanisms, potentially counteracting the effects of slight density reduction and increased overall porosity on shielding performance. Future studies will focus on more comprehensive statistical analyses to confirm these findings definitively.

• To further optimize the performance of CW-incorporated mortars and comprehensively understand their behavior, future studies will systematically investigate the effect of CW fineness (e.g., similar to or finer than cement) and explore mixture designs based on constant workability rather than a constant water-binder ratio, allowing for the evaluation of changes in water demand. These steps are crucial for developing more robust and predictable cementitious composites with colemanite waste.

DECLARATIONS

Acknowledgements: This work was supported by the Scientific Research Projects Coordination Unit of Kırşehir Ahi Evran University (Grant number: MMF.A3.22.011). The authors appreciate the Scientific Research Projects Coordination Unit of Kırşehir Ahi Evran University that supported this study.

Author Contributions: Şevki Eren: Writing, Methodology, Investigation, original draft, Data curation, Funding acquisition, **Doğan Yaşar:** Writing, Methodology, Data curation, **Selahattin Güzelküçük:** Methodology, Data curation, **Gökhan Ekincioğlu:** Methodology, Data curation, **Yunus Karataş:** Methodology, Editing.

Conflict of Interest Disclosure: The authors declare no conflict of interest.

Funding: This work was supported by the Scientific Research Projects Coordination Unit of Kırşehir Ahi Evran University (Grant number: MMF.A3.22.011).

Plagiarism Statement: This article has been evaluated for plagiarism, and no instances of plagiarism were detected.

Availability of Data and Materials: Data will be made available on request.

Use of AI Tools: The authors declare that no Artificial Intelligence (AI) tools were used in the creation of this article.

V. REFERENCES

Aksoğan, O., Binici, H., & Ortlek, E. (2016). Durability of concrete made by partial replacement of fine aggregate by colemanite and barite and cement by ashes of corn stalk, wheat straw and sunflower

stalk ashes. *Construction and Building Materials*, *106*, 253–263. https://doi.org/10.1016/j.conbuildmat.2015.12.102

Al-Saadi, A. J., & Saadon, A. K. (2014). Gamma ray attenuation coefficients for lead oxide and iron oxide reinforced in silicate glasses as radiation shielding windows. *Ibn Al-Haitham Journal for Pure & Applied Sciences, 27*(3), 201–214. https://jih.uobaghdad.edu.iq/index.php/j/article/view/282

Binici, H., Aksogan, O., Sevinc, A. H., & Kucukonder, A. (2014). Mechanical and radioactivity shielding performances of mortars made with colemanite, barite, ground basaltic pumice and ground blast furnace slag. *Construction and Building Materials*, *50*, 177–183. https://doi.org/10.1016/j.conbuildmat.2013.09.033

Castro, J., Bentz, D., & Weiss, J. (2011). Effect of sample conditioning on the water absorption of concrete. *Cement and Concrete Composites*, *33*(8), 805–813. https://doi.org/10.1016/j.cemconcomp.2011.05.007

Demir, D., & Keleş, G. (2006). Radiation transmission of concrete including boron waste for 59.54 and 80.99 keV gamma rays. *Nuclear Instruments and Methods in Physics Research Section B: Beam Interactions with Materials and Atoms*, *245*(2), 501–504. https://doi.org/10.1016/j.nimb.2005.11.139

Demir, F., Budak, G., Sahin, R., Karabulut, A., Oltulu, M., & Un, A. (2011). Determination of radiation attenuation coefficients of heavyweight-and normal-weight concretes containing colemanite and barite for 0.663 MeV γ-rays. *Annals of Nuclear Energy*, *38*(6), 1274–1278. https://doi.org/10.1016/j.anucene.2011.02.009

El-Sayed Abdo, A. (2002). Calculation of the cross-sections for fast neutrons and gamma-rays in concrete shields. *Annals of Nuclear Energy*, *29*(16), 1977–1988. https://doi.org/10.1016/S0306-4549(02)00019-1

Ersundu, A. E., Büyükyıldız, M., Ersundu, M. Ç., Şakar, E., & Kurudirek, M. (2018). The heavy metal oxide glasses within the WO3-MoO3-TeO2 system to investigate the shielding properties of radiation applications. *Progress in Nuclear Energy*, *104*, 280–287. https://doi.org/10.1016/j.pnucene.2017.10.008

Han, B., Zhang, L., & Ou, J. (2017). *Smart and multifunctional concrete toward sustainable infrastructures*. Springer.

International Atomic Energy Agency. (2011). *Radiation protection and safety of radiation sources: International basic safety standards* (N.G. Part, Interim ed.). https://regelwerk.grs.de/sites/default/files/cc/dokumente/dokumente/DS379%20Draft5.0-21Mar2011.pdf

International Commission on Radiological Protection. (2007). *The 2007 recommendations of the International Commission on Radiological Protection (ICRP Publication 103). Annals of the ICRP, 37*(2–4), 1–133.

International Organization for Standardization. (2019). Radiological protection — *X and gamma reference radiation for calibrating dosemeters and doserate meters and for determining their response as a function of photon energy – Part 1: Radiation characteristics and production methods* (ISO 4037-1 :2019(E)). https://cdn.standards.iteh.ai/samples/66872/21db762a1fc9481fb9a84f765cc27afc/ISO-4037-1-2019.pdf

Kavas, T., Olgun, A., Erdogan, Y., & Once, G. (2007). The effect of pectin on the physicochemical and mechanical properties of cement containing boron. *Building and Environment*, *42*(4), 1803–1809. https://doi.org/10.1016/j.buildenv.2006.01.018

Kavaz, E., Ekinci, N., Tekin, H. O., Sayyed, M. I., Aygün, B., & Perişanoğlu, U. (2019). Estimation of gamma radiation shielding qualification of newly developed glasses by using WinXCOM and MCNPX code. *Progress in Nuclear Energy*, *115*, 12–20. https://doi.org/10.1016/j.pnucene.2019.03.029

Khan, F. M., & Gibbons, J. P. (2014). *Khan's the physics of radiation therapy* (5th ed.). Lippincott Williams & Wilkins.

Lotti, P., Comboni, D., Gigli, L., Carlucci, L., Mossini, E., Macerata, E., Mariani, M., & Gatta, G. D. (2019). Thermal stability and high-temperature behavior of the natural borate colemanite: An aggregate in radiation-shielding concretes. *Construction and Building Materials*, *203*, 679–686. https://doi.org/10.1016/j.conbuildmat.2019.01.123

Mehta, P. K., & Monteiro, P. J. (2006). *Concrete: Microstructure, properties, and materials* (3rd ed.). McGraw-Hill.

Mutuk, T., & Mesci, B. (2014). Analysis of mechanical properties of cement containing boron waste and rice husk ash using full factorial design. *Journal of Cleaner Production*, *69*, 128–132. https://doi.org/10.1016/j.jclepro.2014.01.051

Olgun, A., Kavas, T., Erdogan, Y., & Once, G. (2007). Physico-chemical characteristics of chemically activated cement containing boron. *Building and Environment*, *42*(6), 2384–2395. https://doi.org/10.1016/j.buildenv.2006.06.003

Oto, B., Gür, A., Kaçal, M. R., Doğan, B., & Arasoğlu, A. (2013). Photon attenuation properties of some concretes containing barite and colemanite in different rates. *Annals of Nuclear Energy*, *51*, 120–124. https://doi.org/10.1016/j.anucene.2012.06.033

Oto, B., Madak, Z., Kavaz, E., & Yaltay, N. (2019). Nuclear radiation shielding and mechanical properties of colemanite mineral doped concretes. *Radiation Effects and Defects in Solids*, *174*(9–10), 899–914. https://doi.org/10.1080/10420150.2019.1668390

Ouda, A. S. (2015). Development of high-performance heavy density concrete using different aggregates for gamma-ray shielding. *Progress in Nuclear Energy*, *79*, 48–55. https://doi.org/10.1016/j.pnucene.2014.11.009

Öztürk, B. C., Kızıltepe, C. Ç., Ozden, B., Güler, E., & Aydın, S. (2020). Gamma and neutron attenuation properties of alkali-activated cement mortars. *Radiation Physics and Chemistry*, *166*, Article 108478. https://doi.org/10.1016/j.radphyschem.2019.108478

Rezaei-Ochbelagh, D., & Azimkhani, S. (2012). Investigation of gamma-ray shielding properties of concrete containing different percentages of lead. *Applied Radiation and Isotopes*, *70*(10), 2282–2286. https://doi.org/10.1016/j.apradiso.2012.06.020

Saudi, H. A. (2013). Lead phosphate glass containing boron and lithium oxides as a shielding material for neutron and gamma radiation. *Applied Mathematics and Physics*, *1*(4), 143–146. https://doi.org/10.12691/amp-1-4-7

International Electrotechnical Commission. (2014). *Protective devices against diagnostic medical X-radiation – Part 1: Determination of attenuation properties of materials* (IEC 61331-1). https://cdn.standards.iteh.ai/samples/19083/028b83ae94cd4877bfdd8c081dfbf1b2/IEC-61331-1-2014.pdf

Tyagi, G., Singhal, A., Routroy, S., Bhunia, D., & Lahoti, M. (2020). A review on sustainable utilization of industrial wastes in radiation shielding concrete. *Materials Today: Proceedings*, *32*(4), 746–751. https://doi.org/10.1016/j.matpr.2020.03.474

Ustabas, I. (2024). Effect of boron minerals colemanite and ulexite on physical, chemical and mechanical properties of cement. *Sustainability and Clean Building*, *1*(1), 66–78. https://doi.org/10.37256/scb.1120244960

Yadollahi, A., Nazemi, E., Zolfaghari, A., & Ajorloo, A. M. (2016). Optimization of thermal neutron shield concrete mixture using artificial neural network. *Nuclear Engineering and Design*, *305*, 146–155. https://doi.org/10.1016/j.nucengdes.2016.05.012

Yaltay, N., Ekinci, C. E., Çakır, T., & Oto, B. (2015). Photon attenuation properties of concrete produced with pumice aggregate and colemanite addition in different rates and the effect of curing age to these properties. *Progress in Nuclear Energy*, *78*, 25–35. https://doi.org/10.1016/j.pnucene.2014.08.002